Journal of Alloys and Compounds 506 (2010) 788–793

Contents lists available at ScienceDirect

Journal of Alloys and Compounds

journal homepage: www.elsevier.com/locate/jallcom

Physical properties of Ga-doped ZnO thin films by spray pyrolysis

T. Prasada Rao, M.C. Santhosh Kumar*

Advanced Materials laboratory, Department of Physics, National Institute of Technology, Tiruchirappalli 620 015, India

ARTICLE INFO

Article history:
Received 22 December 2009
Received in revised form 7 July 2010
Accepted 8 July 2010
Available online 16 July 2010

PACS:
71.55.Gs
73.61.Ga
78.40.Fy
78.40.Pg
78.55.Et
78.66.Hf

Keywords:
Spray pyrolysis
ZnO
Optical properties
RMS strain
Photoluminescence

ABSTRACT

Gallium doped zinc oxide (GZO) thin films were prepared using the simple, flexible and cost-effective spray pyrolysis technique. The physical properties of the films were studied as a function of increasing gallium dopant concentration from 1 to 9 at.%. The films were characterized by various methods to understand their structural, morphological, optical and electrical properties. The X-ray diffraction analysis revealed that the films were polycrystalline in nature having a hexagonal wurtzite type crystal structure with a preferred grain orientation in the (0 0 2) direction. Scanning electron microscopy (SEM) measurements reveal that the surface morphology of the films changes continuously with a decrease in the grain size due to Ga doping. All the films showed nearly 90% of transparency in the entire visible region. A blue shift of the optical band gap was observed with an increase in Ga doping. Room temperature photoluminescence (PL) measurement of the deposited films indicates incorporation of Ga in ZnO lattice. At 3 at.% Ga doping, the film has lowest resistivity of 6.8×10^{-3} cm while the carrier concentration is highest.

1. Introduction

Zinc oxide (ZnO) is the subject of increasing interest in the last few years owing to its potential applications in ultraviolet (UV) optoelectronic devices [1,2], transparent conducting oxide (TCO) thin films [3,4] and spintronics [5]. For the design and realization of ZnO-based devices, one of the most relevant issues is doping. This issue is especially important for the applications of ZnO as TCO, which necessarily involves the heavy doping with trivalent elements from the group III. By means of doping, large conductivities combined with large ranges of transparency in the visible (VIS) and near UV range are obtained [6,7]. Much effort has been devoted to the development of an alternative to indium based transparent electrodes because of the scarcity of its principal component, indium. Tin doped indium oxide (ITO) is indeed the most widely used TCO for flat panel display (FPD) or solar cell applications. However, indium is a very expensive material and ITO is less stable in hydrogen plasma. Therefore, impurity doped zinc oxide (ZnO), such as Al or Ga-doped ZnO, has recently gained much attention [8–12] as an alternative material to ITO. Ga-doped ZnO (GZO) is more stable with respect to oxidation due to gallium's greater electronegativity in comparison with aluminium [13]. It has also been reported that heavily Ga-doped ZnO is more stable when subjected to moisture than Al-doped ZnO [14]. Moreover, recent studies have reported the use of ZnO as an air stable anode in an OLED, providing additional evidence of GZO as a promising TCO for organic device applications [15]. It is believed that the introduction of Ga can increase free electron density by replacing the host atoms (Zn) [16]. The substitution of Ga is possible due to the smaller radius of Ga (0.062 nm) compared with Zn (0.083 nm). Several approaches have been proposed and developed for the preparation of Ga-doped ZnO thin films such as magnetron sputtering [17], spray pyrolysis [18], metal-organic chemical vapour deposition (MOCVD) [19], pulsed laser deposition (PLD) [20], arc plasma evaporation [21], dip-coating [22] and ion plating [23]. Among these, spray pyrolysis is one of the most used methods. Spray pyrolysis has been developed as a powerful tool to prepare various kinds of thin films such as metal oxides, superconducting materials, and nanophase materials. In comparison with other chemical deposition techniques, spray pyrolysis has several advantages such as high purity, excellent control of chemical uniformity, and stoichiometry in multi-component system. Other advantages of the spray pyrolysis method are that it can be adapted easily for production of large-area films, and to get varying band gap materials during the deposition process.

* Corresponding author: Tel.: +91 9443834014; fax: +91 04312500133.
E-mail addresses: prasadview@gmail.com (T. Prasada Rao), santhoshmc@nitt.edu, santhoshmc@yahoo.com (M.C. Santhosh Kumar).

0925-8388/$ – see front matter © 2010 Elsevier B.V. All rights reserved.
doi:10.1016/j.jallcom.2010.07.071

In this work, we report the structural, optical and electrical properties of the transparent conducting GZO thin films prepared by spray pyrolysis method. We sought optimum deposition conditions yielding GZO films with desired physical properties, specifically good crystalline quality microstructure, low resistivity and high transparency.

2. Experimental details

Spray pyrolysis is an effective method for the deposition of thin films of metallic oxides, as is the case with the GZO material. The precursor solution for spray pyrolysis was prepared by dissolving an appropriate amount of zinc acetate dihydrate and gallium nitrate in the mixture of deionized water and ethanol at room temperature. In this mixture, ethanol concentration was 10 ml in 100 ml solution. A few drops of acetic acid were added to aqueous solutions to prevent the formation of hydroxides. The concentration of gallium was varied from 1 to 9 at.%. The total concentration of the solution was maintained at 0.1 mol l^{-1}. The glass substrates were cleaned thoroughly with acetone, isopropanol and finally with deionized water with the help of an ultrasonic bath. The nozzle was at a distance of 20 cm from the substrate during deposition. The solution flow rate was held constant at 3 ml/min. Air was used as the carrier gas, at the pressure of 2 bar. When aerosol droplets close to the substrates, a pyrolytic process occurs and highly adherent GZO films were produced. The GZO thin films were deposited at substrate temperature at 623 K with 200 nm thickness.

The thickness was measured using Stylus profile meter. The structural properties were studied by X-ray diffraction measurements (XRD) using Rigaku D/Max ULTIMA III diffractometer with CuK_α radiation ($\lambda = 1.5406$ Å). The average dimensions of crystallites were determined by the Scherrer method from the broadening of the diffraction peaks. The optical measurements of the ZnO thin films were carried out at room temperature using shimadzu UV-1700 Spectrophotometer in the wavelength range 300–1100 nm. PL measurements were performed using the 325 nm line from a Xenon pulse lamp as the excitation source and a UV–vis photomultiplier tube were used to detect the PL signals. JEOL JSM 35 electron microscope was used to record SEM micrographs. Electrical properties, namely resistivity, Hall mobility, and carrier concentration were measured at room temperature using a standard Hall measurement system (Ecopia, Model: HMS-3000) in van der Pauw configuration.

3. Results and discussion

3.1. Structural characteristics

Fig. 1 shows the XRD patterns of the as-prepared ZnO thin films doped with different Ga concentrations. All the films show the existence of a very strong peak corresponding to (0 0 2) and weak peaks corresponding to (1 0 0), (1 0 1) reflections of the wurtzite phase of ZnO. Apart from ZnO characteristic peaks, no peaks that correspond to either gallium, zinc or their complex oxides could be detected. This observation suggests that the films do not have any phase segregation or secondary phase formation. It is also observed that the full width at half maximum (FWHM) of the peak corresponding to the (0 0 2) reflection increases with Ga incorporation in the films. The FWHM value increases from 0.1333° to 0.1759° as Ga doping concentration increases from 1 to 9 at.%. These results indicate that increasing Ga doping concentration could degrade the crystallinity of the GZO films due to small crystallites in the films. The crystallite size '*P*' is calculated using Scherrer's formula [24,25]:

$$P = \frac{0.94\lambda}{\beta \cos\theta} \tag{1}$$

where β is the broadening of the diffraction line (FWHM) and λ is the X-ray wavelength. The instrumental broadening effect has been removed by using the XRD pattern of a standard silicon sample. It is seen that as doping increases the crystallite size decreases up to 9 at.% as shown in Table 1. The preferential or random growth of polycrystalline thin films can be understood from calculating the texture coefficient TC (*h k l*) for all planes. The texture coefficient is calculated using the following equation [25]:

$$TC(hkl) = \left(\frac{I_{(hkl)}/I_{r(hkl)}}{\left[1/n \sum I_{(hkl)}/I_{r(hkl)}\right]} \right) \tag{2}$$

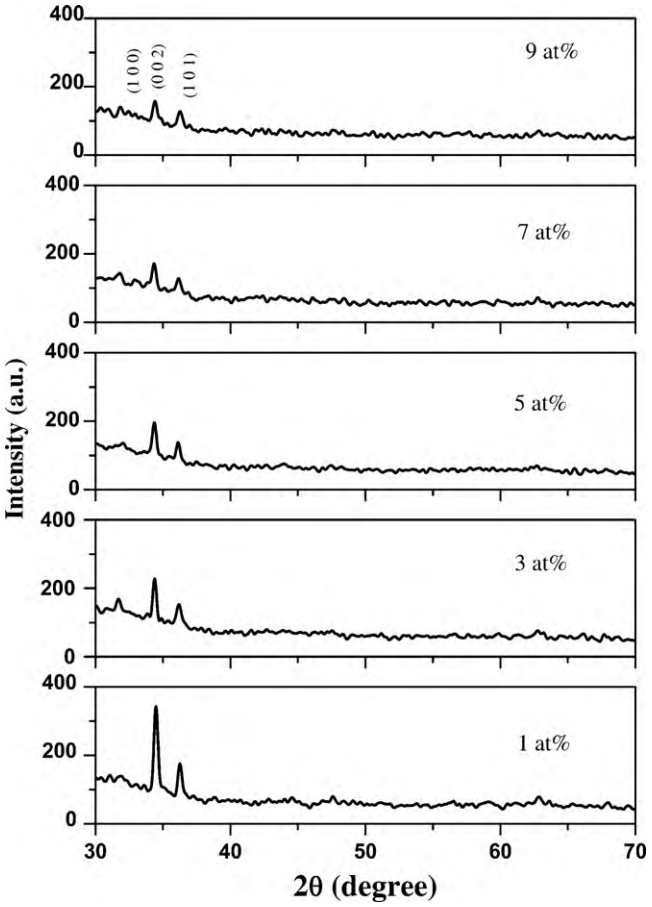

Fig. 1. XRD patterns of GZO thin films with various Ga concentrations.

where $I_{(hkl)}$ indicate the X-ray diffraction intensities obtained from the films, and n is the number of reflections observed in the XRD pattern. $I_{r(hkl)}$ is the intensity of the reference diffraction pattern(JCPDS card 75-0576). It is clear from the definition that the deviation of texture coefficient from unity implies the film growth in preferred orientation. Table 1 shows the variation of the texture coefficient with variation of Ga doping concentration for the (0 0 2) plane. The texture coefficient for all the films has a relatively (>1) higher value along the (0 0 2) plane. It can be concluded that the crystallites are preferentially oriented along the (0 0 2) plane. Moreover, the intensity of the (0 0 2) peak gradually decreases with the increase in the Ga content in the films. This behaviour indicates that the increase in the doping concentration deteriorates the crystallinity of the films, which may be attributed to the influence of stresses arising from the difference in the ionic radii of zinc and gallium [26]. Assuming that the broadening of the diffraction peak ($W_{2\theta}$) is due to both crystallite size and strain, the variance of 2θ values can be written as

$$W_{2\theta} = \left[\frac{\lambda\sigma}{2\Pi^2 P \cos\theta}\right] + 4\tan^2\theta \left\langle \varepsilon^2 \right\rangle \tag{3}$$

where σ is the angular range over which the intensity is appreciable and $\langle\varepsilon^2\rangle$ is the mean squared strain. Dislocation density 'ρ' is defined as the length of the dislocation lines per unit volume of the crystal [27]. Williamson and Smallman [28] suggested a method of calculating the dislocation density using the expression:

$$\rho = \left[\frac{\sqrt{12}\left\langle \varepsilon^2 \right\rangle^{1/2}}{Pd}\right] \tag{4}$$

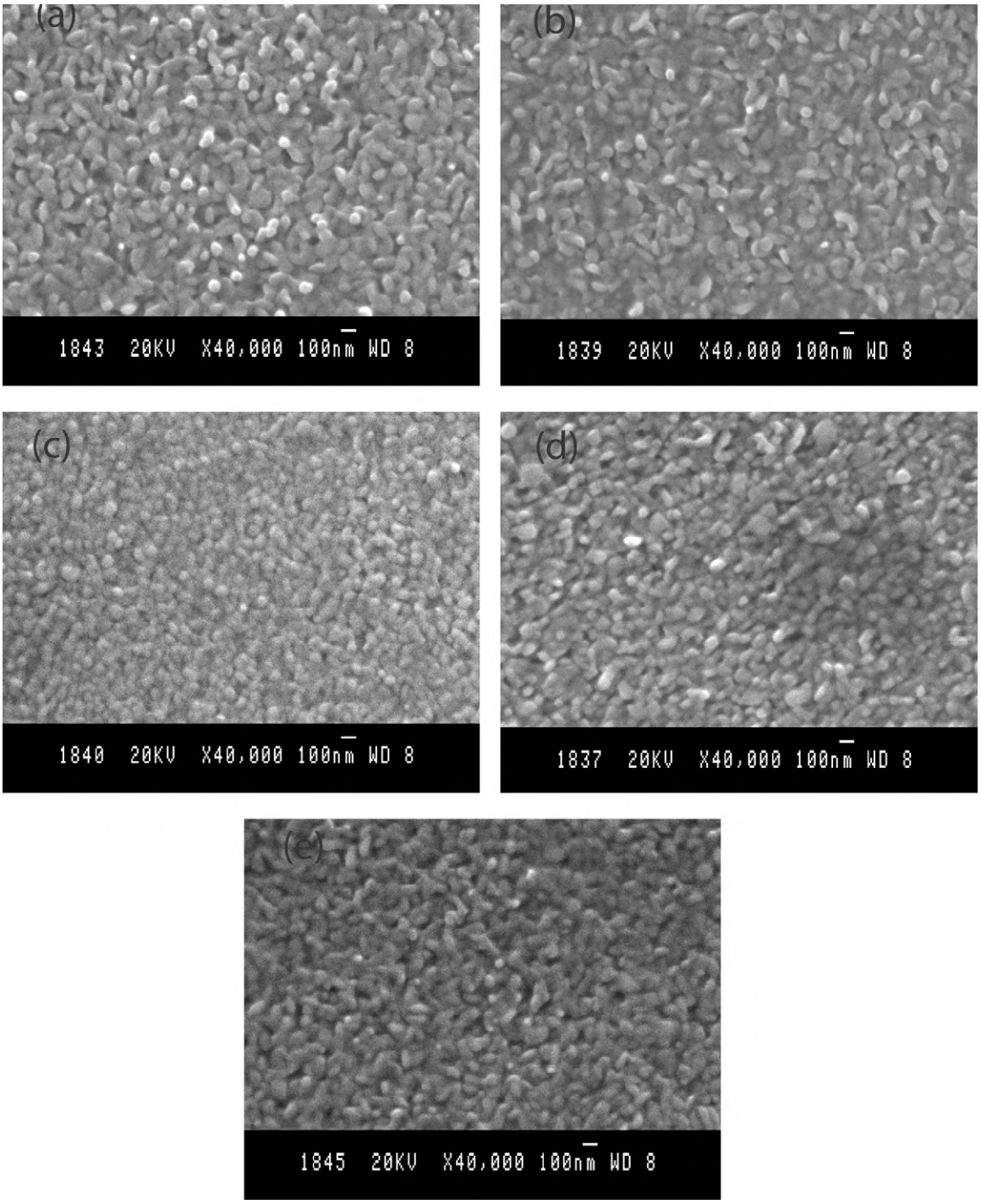

Fig. 2. SEM picture of (a) 1%; (b) 3%; (c) 5%; (d) 7%; (e) 9% Ga doped.

where $\langle \varepsilon^2 \rangle^{1/2}$ is the root mean squared (rms) strain. The rms strain is evaluated using Eqs. (3) and (4). Table 1 shows the variations of crystallite size and rms strain for GZO thin films with respect to Ga doping %. It is clear from Table 1 that the films grown at 1 at.% exhibited the least rms strain and the greatest crystallite size.

Fig. 2 shows the surface morphology of GZO films with different Ga concentrations. It shows a uniform grain growth in all samples. The particulates (grains) are small and distributed uniformly throughout the surface. As Ga doping concentration increases up to 9 at.%, a gradual decrease in crystallite size occurred due to an increasing number of nucleation centres during incorporation of the dopant into the host material [29]. Thus the SEM analysis corroborates the XRD studies.

3.2. Optical properties

Fig. 3 shows the transmittance spectra obtained for the GZO films. The transmittance measurements reveal that the films are highly transparent in the visible region. The decrease in transmittance at higher doping concentrations may be due to the increased scattering of photons by crystal defects created by doping. All the samples exhibit a transmittance peak in UV region (295–370 nm) just before the absorption edge. This peak is found to increase with

Table 1
Calculated d, TC, FWHM, particle size, rms strain, ρ, E_g and E_{Urb} values of GZO thin films.

Dopant (at%)	d (Å)	TC (0 0 2)	FWHM (°)	Particle size (nm)	rms strain $(\langle\varepsilon^2\rangle^{1/2})$	ρ (line/m^2) $\times 10^{16}$	Band gap E_g (eV)	E_{Urb} (mev)
1	2.5961	1.66	0.1333	65	0.5874	12.06	3.249	58.16
3	2.6093	1.58	0.1395	62	0.6044	12.94	3.265	61.04
5	2.6093	1.57	0.1421	61	0.6100	13.27	3.275	63.96
7	2.6093	1.51	0.1566	55	0.6415	15.49	3.282	65.03
9	2.6226	1.52	0.1759	48	0.6824	18.78	3.290	72.09

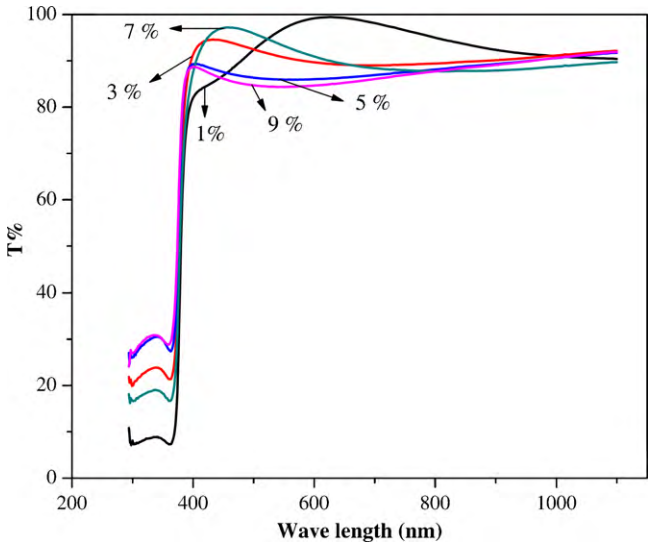

Fig. 3. Optical transmittance spectrum of Ga-doped ZnO thin films.

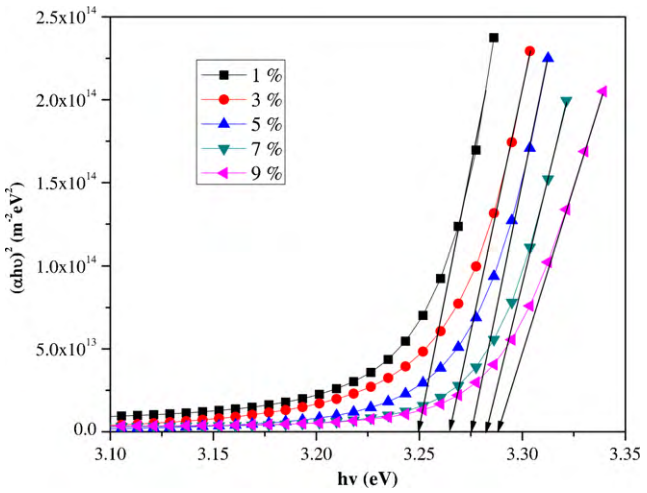

Fig. 4. Variation of $(\alpha h\upsilon)^2$ versus $h\upsilon$ of the GZO thin films.

doping concentration. This may be attributed to the decrease in crystallinity of the GZO thin films. All these samples have band edge near to 373 nm corresponding to ZnO. It has also been observed that the absorption edge shows a blue shift with Ga concentration. The absorption coefficient α is deduced from T using the Beer–Lambert law:

$$\alpha = \frac{1}{t}\ \ln\left[\frac{1}{T}\right] \tag{5}$$

where t is the film thickness. Tauc's theory for the direct allowed transitions such as those occurring in the direct gap of ZnO approximates α near the band edge to

$$\alpha h\upsilon = A\sqrt{h\upsilon - E_g} \tag{6}$$

where A is a constant and $h\nu$ is the incident photon energy. The optical energy gap E_g of the films can be now estimated by extrapolating the linear part of the $(\alpha h\nu)^2$ to the $h\nu$-axis of the Tauc's plot shown in Fig. 4. The optical band gap increases from 3.24 to 3.29 eV with gallium doping concentration. The change in the optical band gap can be explained in terms of Burstein–Moss band gap widening [29]. According to the Burstein–Moss effect, the increase in the Fermi level in the conduction band leads to the band gap energy broadening with increasing carrier concentration. The band gap energy determined in this way is not the actual band gap of the deposit. As these are degenerate semiconductors, the Fermi level lies within the conduction band where its position depends on the density of the free electrons. Thus, the values given for the optical band gaps are related to the excitation of the electrons from the valance band to the Fermi level in the conduction band, whereas the actual band gap of the material is related to the excitation of the electrons from the top of the valence band to the bottom of the conduction band. This means that the lifting of the Fermi level into the conduction band of the degenerate semiconductor due to the increase in the carrier density leads to the energy band broadening (shifting) [30]. The absorption below E_g is described by

$$\alpha = \alpha_0\ \exp\left(\frac{h\upsilon}{E_{Urb}}\right) \quad \text{for} \quad h\upsilon < E_g \tag{7}$$

where the Urbach energy parameter E_{Urb} is deduced from the plot of $\ln(\alpha)$ versus $h\nu$ (Fig. 5). According to the Urbach absorption tail model, the material absorption edge band gap is due to states created by defects and disorder in materials. The Urbach energy E_{Urb} increases from 58 to 72 meV as doping is raised from 1 to 9 at.%, indicating the film structural disorder and defects with Ga doping. This supports the earlier observations of XRD.

Room temperature PL emission spectrum for all the samples was measured in the wavelength range 350–650 nm at an excitation wavelength of 325 nm. PL spectra of the GZO thin films are

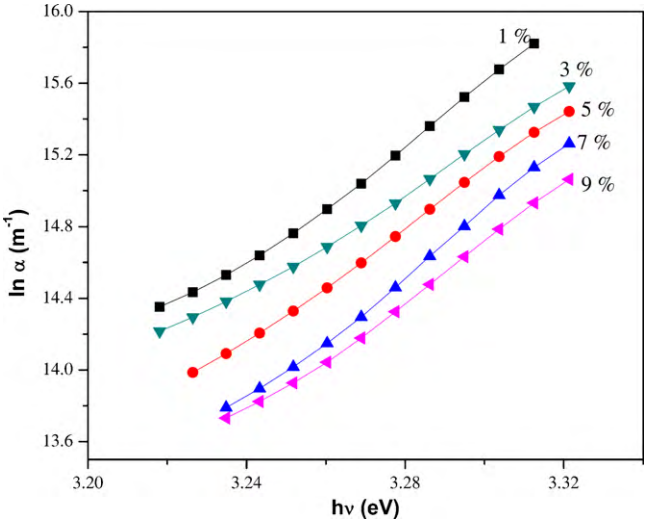

Fig. 5. $\ln(\alpha)$ versus $h\upsilon$ of GZO thin films.

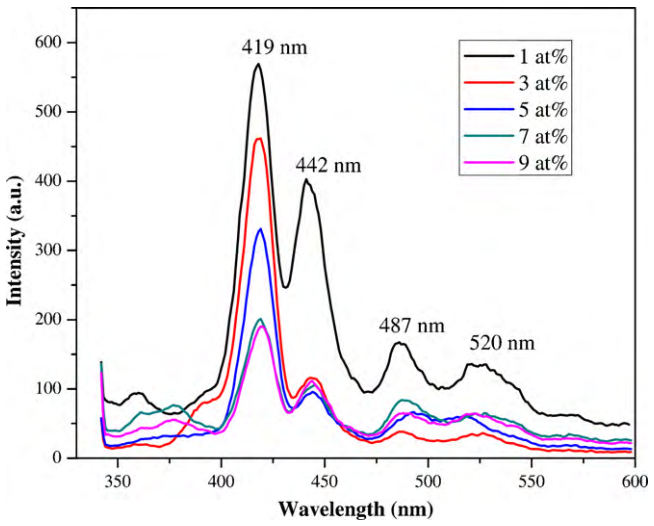

Fig. 6. Photoluminescence emission spectrum of ZnO thin films with various Ga concentrations.

shown in Fig. 6. Four emissions peaks at 419, 442, 487 and 520 nm appeared in the PL spectra of the GZO films. The emission spectra show a strong violet emission band around 415–420 nm in all samples. This violet peak can be attributed to the Zn vacancies [31,32]. The intensity of the band-edge emission peak gradually decreases with the increase in Ga content in the films. Similar behaviour has also been observed by Kaul et al. [19] for Ga-doped ZnO prepared by MOCVD. The PL spectrum of the undoped ZnO film shows a very broad feature below 520 nm due to the presence of interstitial oxygen defects in ZnO films [33]. However, the broad feature disappears in the case of Ga-doped ZnO films, which may be due to the consumption of interstitial oxygen by Ga^{3+} ions. PL studies on Ga-doped ZnO thin films showed a drastic decrease in the intensity of the blue-green emission (Fig. 6). The violet emission at 419 nm was probably due to the radiative defects related to the interface traps existing at the grain boundaries and the emission was due to the transition between this level and the valence band [32]. When gallium was doped in the film, it was assumed that, gallium occupied in the zinc lattice site, reducing the probability of forming oxygen vacancies. Hence the density of oxygen vacancies would be less in the film. This might be the reason for the decrease in intensity of the blue-green emission with Ga concentration.

3.3. Electrical properties

In an earlier communication we have reported the electrical resistivity value of $5.27 \times 10^3\ \Omega$ cm and mobility value of $0.20\ cm^2/V\,s$ for the undoped ZnO films [34]. The electrical properties of Ga-doped ZnO thin films drastically improved in comparison with undoped ZnO thin films. Table 2 shows the variation of carrier concentration, carrier mobility and electrical resistivity with the various percentages (at.%) of Ga doping in the GZO thin films deposited by spray pyrolysis. At 3 at.% Ga doping, the film has lowest resistivity of $6.8 \times 10^{-3}\ \Omega$ cm while the carrier concentration is highest. The increased carrier concentration caused by Ga doping reduces the grain boundary potential barrier, which reduces the resistivity. The decrease in resistivity with different dopant concentrations is attributed to the replacement of Zn^{2+} by Ga^{3+} ions which introduce a large number of electrons in the doped films. Thus, the conductivity of the film increases. However, further increase in Ga doping to above 3 at.% raised the resistivity and reduced the carrier concentration. This may be understood from the two reasons. At a higher doping concentration of above 3 at.%, the disorder produced in the lattice (due to difference in the ionic radii of Zn^{2+} and Ga^{3+}) increases the efficiency of scattering mechanism such as phonon scattering and ionized impurity scattering which, in turn, causes an increase in resistivity [35]. This is consistent with the result of structural studies in the sense that the lattice strain is found to be higher (shown in Table 1) in case of the heavily doped films because of the lattice disorder. The other reason is the segregation of neutral Ga atoms at the grain boundaries in heavily doped samples which do not contribute free electrons [36]. The electrical measurements were performed several times on all the samples, and much the same results were obtained in each case. According to previous reports [36–41] the optimal value of Ga dopant concentration marginally vary from 2 to 3 at.%. Moreover it is found to depend on the preparation technique and experimental conditions. In the present study we observed that 3 at.% is the optimum value of Ga in ZnO to obtain good electrical properties.

Table 2
Restivity, carrier concentration and mobility values of GZO thin films.

Ga (at.%)	Resistivity (Ω cm)	Carrier concentration (cm^{-3})	Mobility ($cm^2/V\,s$)
1	9.0×10^{-3}	2.64×10^{19}	26.3
3	6.8×10^{-3}	3.14×10^{19}	29.2
5	8.4×10^{-3}	2.68×10^{19}	27.6
7	9.3×10^{-3}	2.55×10^{19}	26.3
9	9.8×10^{-3}	2.50×10^{19}	25.5

4. Conclusion

Ga-doped ZnO (GZO) films were deposited on amorphous glass substrates at 623 K by spray pyrolysis. The physical properties of these films have been studied in detail as a function of increasing Ga doping (from 1 to 9 at.%) concentration. The XRD analysis showed that GZO films possess polycrystalline hexagonal wurtzite structure with a preferred orientation along the (0 0 2) direction. With the increase in Ga concentration, the rms strain of the films has increased. Simultaneously, the grain orientation in the (0 0 2) axis decreased with an increase in the FWHM value (indication of smaller grains). The SEM measurements showed that, upon increasing the Ga concentration, the surface morphology of the films is uniform and grains are distributed uniformly throughout the surface. Optical transmittance measurements showed a substantial blue shift of the band gap, which can be interpreted in terms of band gap modulation due to Ga doping. With the increase in Ga concentration, the band gap of the films increased from 3.24 to 3.29 eV. The optical and electrical characterization studies clearly indicate the incorporation of Ga into ZnO. Hence the observed increase in the optical band gap and the variation in electrical resistivity can be directly attributed to the effect of Ga ion incorporation into the ZnO lattice. At 3 at.% Ga doping, the film has lowest resistivity of $6.8 \times 10^{-3}\ \Omega$ cm while the carrier concentration is highest. From our experiments we have demonstrated that the physical properties of ZnO can be well modified by gallium doping.

Acknowledgement

Authors are thankful to the Director, National Institute of Technology, Tiruchirappalli for providing financial support for this work through the TEQIP networking project.

References

[1] H. Ohta, K. Kawamura, M. Orita, N. Sarukura, M. Hirano, H. Hosono, Electron. Lett. 36 (2000) 984–985.
[2] X.L. Guo, J.H. Choi, H. Tabata, T. Kawai, Jpn. J. Appl. Phys. 40 (2) (2001) L177–L180.

[3] V. Assunção, E. Fortunato, A. Marques, A. Gonçalves, I. Ferreira, I. Águas, R. Martins, Thin Solid Films 442 (2003) 102–106.
[4] S.J. Henley, M.N.R. Ashfold, D. Cherns, Surf. Coat. Technol. 177 (2004) 271–276.
[5] F. Pan, C. Song, X.J. Liu, Y.C. Yang, F. Zeng, Mater. Sci. Eng. R 62 (2008) 1–35.
[6] B.E. Sernelius, K.F. Berggren, Z.C. Jin, I. Hamberg, C.G. Granqvist, Phys. Rev. B 37 (1988) 10244–10248.
[7] H. Fujiwara, M. Kondo, Phys. Rev. B 71 (2005), 075109-1-10.
[8] V. Bhosle, A. Tiwari, J. Narayan, Appl. Phys. Lett. 88 (2006), 032106-1-3.
[9] C. Guillĩen, J. Herrero, Thin Solid Films 515 (2006) 640–643.
[10] P. Nunes, E. Fortunato, P. Tonello, F.B. Fernandes, P. Vilarinho, R. Martins, Vacuum 64 (2002) 281–285.
[11] S.B. Majumder, M. Jain, P.S. Dobal, R.S. Katiyar, Mater. Sci. Eng. B 103 (2003) 16–25.
[12] H. Kim, C.M. Gilmore, J.S. Horwitz, A. Piquĩe, H. Murata, G.P. Kushto, R. Schlaf, Z.H. Kafafi, D.B. Chrisey, Appl. Phys. Lett. 76 (2000) 259–261.
[13] K. Yim, H.W. Kim, C. Lee, Mater. Sci. Technol. 23 (2007) 108–112.
[14] O. Nakagawara, Y. Kishimoto, H. Seto, Y. Koshido, Y. Yoshino, T. Makino, Appl. Phys. Lett. 89 (2006), 091904-1-3.
[15] H.J. Bolink, E. Coronado, D. Repetto, M. Sessolo, Appl. Phys. Lett. 91 (2007) 223501–223503.
[16] J. Hu, R.G. Gordon, J. Appl. Phys. 72 (1992) 5381–5392.
[17] Q.B. Ma, Z.Z. Ye, H.P. He, S.H. Hu, J.R. Wang, L.P. Zhu, Y.Z. Zhang, B.H. Zhao, J. Cryst. Growth 304 (2007) 64–68.
[18] K.T.R. Reddy, T.B.S. Reddy, I. Forbes, R.W. Miles, Surf. Coat. Technol. 151 (2002) 110–113.
[19] A.R. Kaul, O.Y. Gorbenko, A.N. Botev, L.I. Burova, Superlatt. Microstruct. 38 (2005) 272–282.
[20] M. Snure, A. Tiwari, J. Appl. Phys. 101 (2007) 124912–124916.
[21] T. Minami, S. Ida, T. Miyata, Y. Minamino, Thin Solid Films 445 (2003) 268–273.
[22] V. Fathollahi, M.M. Amini, Mater. Lett. 50 (2001) 235–239.
[23] K. Iwata, T. Sakemi, A. Yamada, P. Fons, K. Awai, T. Yamamoto, M. Matsubara, H. Tampo, S. Niki, Thin Solid Films 445 (2003) 274–277.
[24] T. Prasada Rao, M.C. Santhosh Kumar, Appl. Surf. Sci. 255 (2009) 4579–4584.
[25] T. Prasada Rao, M.C. Santhosh Kumar, Appl. Surf. Sci. 255 (2009) 7212–7215.
[26] J. Nishino, S. Ohshio, K. Kamata, J. Am. Ceram. Soc. 75 (1992) 3469–3472.
[27] B.E. Warren, E.P. Warekois, Acta Metall. 3 (1955) 473–479.
[28] G.K. Williamson, R.E. Smallman, Phil. Mag. 1 (1956) 34–46.
[29] R.A. Smith, Semiconductors, Academic Publishers, Calcutta, 1989, pp. 461–463.
[30] R. Ferro, J.A. Rodrĩıguez, Thin Solid Films 347 (1999) 295–298.
[31] S.H. Jeong, B.S. Kim, B.T. Lee, Appl. Phys. Lett. 82 (2003) 2625–2627.
[32] B.J. Jin, S. Im, S.Y. Lee, Thin Solid Films 366 (2000) 107–110.
[33] Y. Liu, J. Lian, Appl. Surf. Sci. 253 (2007) 3727–3738.
[34] T. Prasada Rao, M.C. Santhosh Kumar, A. Safarullaa, V. Ganesan, S.R. Barman, C. Sanjeeviraja, Physica B 405 (2010) 2226–2231.
[35] B. Joseph, P.K. Manoj, V.K. Vaidyan, Ceram. Int. 32 (2006) 487–493.
[36] P.K. Nayak, J. Yang, J. Kim, S. Chung, J. Jeong, C. Lee, Y. Hong, J. Phys. D: Appl. Phys. 42 (2009) 035102.
[37] H. Gomez, A. Maldonado, M. de la, L. Olvera, D.R. Acosta, Solar Energy Mater. Solar Cells 87 (2005) 107–116.
[38] H. Gĩomez, M. de la, L. Olvera, Mater. Sci. Eng. B 134 (2006) 20–26.
[39] A. Tiburcio-Silver, A. Sanchez-Juarez, A. Avila-Garcia, Solar Energy Mater. Solar Cells 55 (1998) 3–10.
[40] Q.-B. Ma, Z.-Z. Ye, H.-P. He, L.-P. Zhu, B.-H. Zhao, Mater. Sci. Semiconduct. Process. 10 (2007) 167–172.
[41] K.T. Ramakrishna Reddy, T.B.S. Reddy, I. Forbes, R.W. Miles, Surf. Coat. Technol. 151–152 (2002) 110–113.